Title
In Situ Microscopy and Spectroscopy Applied to Surfaces at Work

Journal
ChemCatChem, 7(22)

ISSN
1867-3880

Authors
Han, Hui-Ling
Melaet, Gérôme
Alayoglu, Selim
et al.

Publication Date
2015-11-01

DOI
10.1002/cctc.201500642

Peer reviewed

ChemPubSoc Europe
DOI: 10.1002/cctc.201500642
CHEMCATCHEM Reviews

AEM 3

In Situ Microscopy and Spectroscopy Applied to Surfaces at Work

Hui-Ling Han,[a] Gérôme Melaet,[a] Selim Alayoglu,[b] and Gabor A. Somorjai*[b, c]

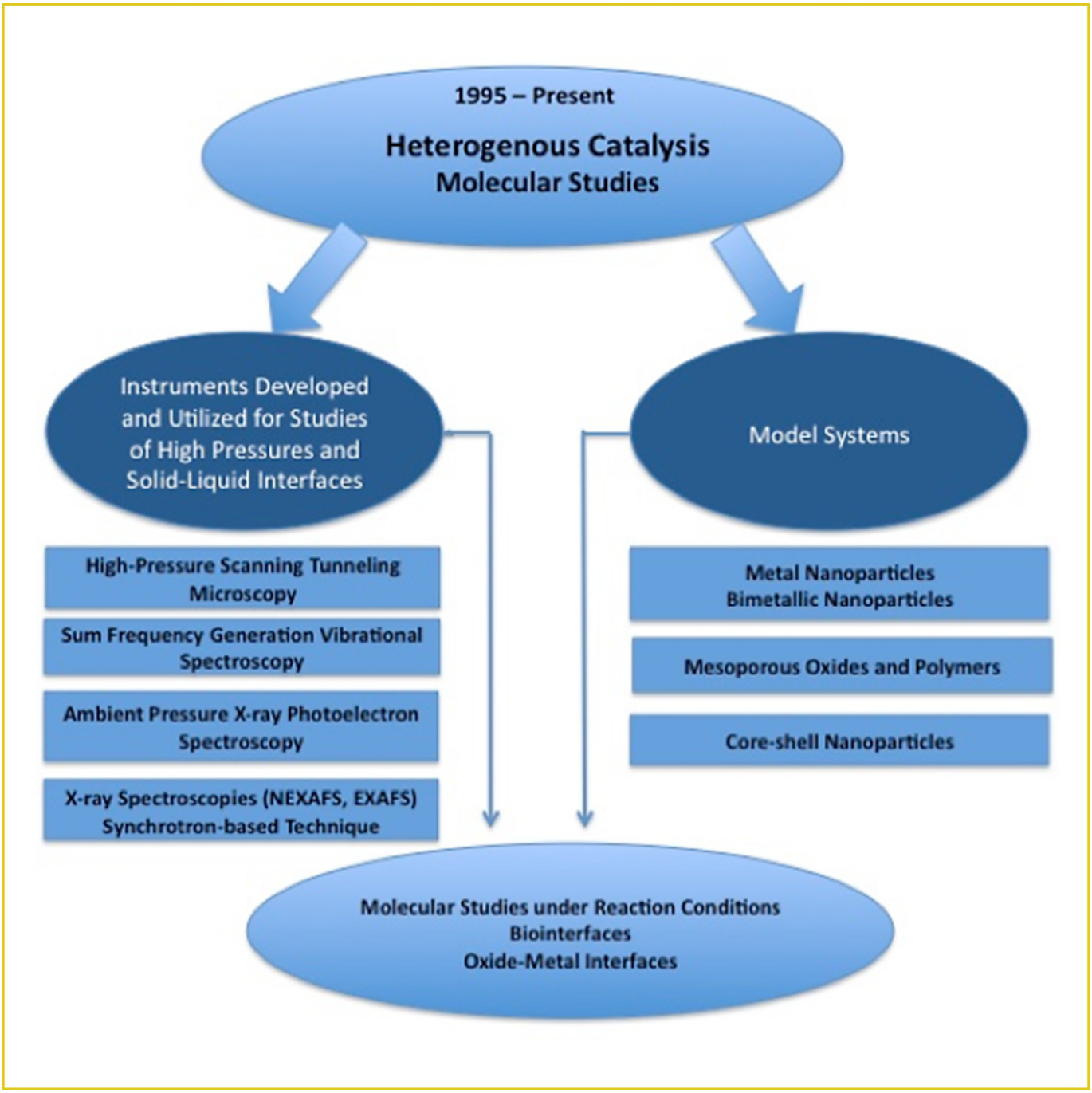

The present review discusses the current state of the art microscopic and spectroscopic characterization techniques available to study surfaces and interfaces under working conditions. Microscopic techniques such as environmental transmission electron microscopy and in situ transmission electron microscopy are first discussed showing their applications in the field of nanomaterials and catalysis. Next sum frequency generation vibrational spectroscopy is discussed, giving probing examples of surface studies in gaseous conditions. Synchrotron based X-ray techniques are also examined with a specific focus on ambient pressure X-ray photoelectron and absorption techniques such as near and extended X-ray absorption fine structure. Each of the techniques is evaluated, whilst the pros and cons are discussed in term of surface sensitivity, spatial resolution and/or time resolution. The second part of the articles is articulated around the future of in situ characterization, giving examples of the probable development of the discussed techniques as well as an introduction of emerging tools such as scanning transmission X-ray microscopy, ptychography, and X-ray photon correlation spectroscopy.

Introduction

Catalysis is a paramount tool for the modern chemical industry; the fabrication of more than 85% of all transportation fuels and high value chemicals involves a catalytic step in the production process. Often these catalytic materials consist of one or more nanomaterial (metal or oxide nanoparticles) dispersed on a high surface area solid support. With the catalytic properties and performances of the material being directed by the interaction between gas–solid (reactants/products–active species), and solid–solid (active species–support) interfaces, it is imperative to characterize these complex systems under reactive conditions. Any new findings will provide a better understanding on the nature of the active site, as well as will give tools to help designing catalysts with increased performances such as a "100%" selectivity for multipath reactions. The content of this review is to show the general trends, the latest technical development and implication of in situ techniques in the field of heterogeneous catalysis.

Environmental Transmission Electron Microscopy

The main advantage of typical high vacuum transmission electron microscopy (TEM) is the ability to monitor nanomaterials instead of single crystals. However, the mean free path of electrons is minute at atmospheric pressure, which makes it extremely difficult to study gas–solid interactions under conditions typical of those that prevail in industrial applications. Over the years, however, successful efforts have been made to create environmental or in situ transmission electron microscopy (E-TEM) to monitor solid–gas interactions with high spatial resolution offering a visualization of atoms in real space and time to the field of heterogeneous catalysis.

The early development of the technique involves the post addition of a differential pumping system. Briefly, the gas is dosed in the objective lens area, and a set of pressure limiting apertures at the stages of the objective lens slowly evacuate the gas, while allowing the electrons to travel through the column to the sample.[1,2] This mode allows, depending on the nature of the gas, to study catalytic material under tens of mbar of gas. Beside the evident pressure limitation, this approach presents another obstacle, owing to the use of specific pressure-limiting apertures at the stages of the objective lens: it creates physical constraints diminishing the capabilities of the TEM (i.e. block high angle scattered electron limiting the annular dark-field imaging to low-angle regime). Nevertheless, except from the gas, no physical object interferes with the electron beam during the imaging, therefore, it allows light-element materials to be imaged with high resolution.[3] This type of E-TEM is by far the most widespread and has produced high quality information on important reactions (Figure 1).

For one working in the field of heterogeneous catalysis, one of the first questions that comes to mind is how the nanoparti-

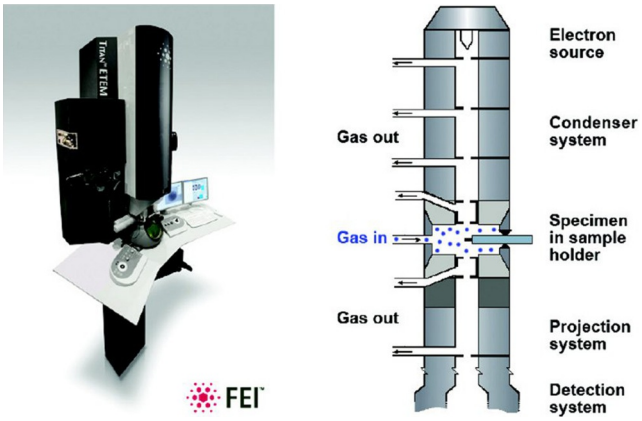

Figure 1. Example of environmental TEM with the Titan ETEM G2 from FEI Company, and the schematic of the microscope column and the differential pumping system.

[a] *Dr. H.-L. Han,[+] Dr. G. Melaet[+]*
Materials Sciences Division
Lawrence Berkeley National Laboratory
1 Cyclotron Road, Berkeley CA 94720 (USA)

[b] *Dr. S. Alayoglu, Prof. Dr. G. A. Somorjai*
Chemical Sciences Division
Lawrence Berkeley National Laboratory
1 Cyclotron Road, Berkeley, CA 94720-8176 (USA)
E-mail: Somorjai@berkeley.edu

[c] *Prof. Dr. G. A. Somorjai*
College of Chemistry
University of California at Berkeley
420 Latimer Hall, Berkeley, CA 94720-1460 (USA)

[+] *These authors contributed equally to this work.*

This publication is part of a Special Issue on Advanced Microscopy and Spectroscopy for Catalysis. Once the full issue has been assembled, a link to its Table of Contents will appear here.

cles structure and morphology changes over a range of different gas compositions and temperatures. For instance, the study by Hansen, on a methanol synthesis catalyst consisting of copper nanoparticles, depicts the dynamic reversible changes of the particles induced by the adsorbate under reactive conditions.[4] Moreover, owing to the ≈0.2 nm spatial resolution, they identified the catalytically active facets on the Cu particles. The time and spatial resolution of in situ TEM has also led to a series of work on the growth of graphite and carbon nanotubes over metal particles.[5–9] Also of interest is the work by Helveg et al. which focuses on the growth of carbon nanofiber from methane and hydrogen on nickel nanocrystals.[10] They have evidenced that the nucleation of graphene starts at mono-atomic step edges while the growth mechanism involves the diffusion of C and Ni atoms.

With the advent of the next TEM generation endow with an aberration corrected lens,[3,11] specific issues of heterogeneous catalysis and processes such as deactivation by "coke" formation,[12] or the importance of metal–support interaction on the performance of supported catalysts,[13,14] could be addressed. For example, Peng et al. showed the growth of a graphene layer on Pt nanoparticles to be a structure-sensitive reaction which depends on the size of the Pt particles supported on MgO.[12] The time resolution also allowed scientists to witness the growth of nanocrystal and nanomaterial at the atomic scale.[15,16] Other effects such as material reconstruction[4,17–20] or particles sintering and ripening[21–24] where successfully evidenced by environmental TEM.

Another approach to in situ TEM is to use a hermetically sealed cell with windows, also called a nanoreactor system (see Figure 2). Practically, the sample is trapped between two

Hui-Ling Han received her Ph.D. in the Department of Applied Chemistry at National Chiao Tung University in Taiwan in 2011 under supervision of Prof. Yuan-Pern Lee. She studied mass selective IR spectroscopy of free radicals and clusters using IR-VUV photoionization techniques during her doctoral research. She studied 2D materials with nonlinear laser spectroscopy techniques during her postdoctoral research in the department of physics in University of California Berkeley. She currently is a postdoctoral researcher in Prof. Gabor Somorjai's group at Lawrence Berkeley National Laboratory, studying surface chemistry under catalytic reaction and electrochemistry on the electrodes of Li batteries with sum frequency generation vibrational spectroscopy.

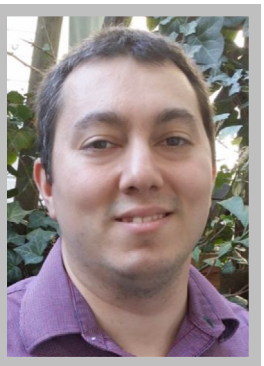

Selim Alayoglu is a scientist in the Chemical Sciences Division with specialization in physical chemistry at Lawrence Berkeley Laboratory. He completed his Ph.D. in chemistry at University of Maryland, College Park, under supervision of Prof. Bryan Eichhorn in 2009. He was a post-doctoral research associate at University of California, Berkeley, under supervision of Prof. Gabor Somorjai until 2014. He is interested in catalysis and chemistry in real-time and under working conditions. More specifically, his work focuses on multi-modal probing of chemical and catalytic transformations using X-ray and optical spectroscopy via microreactors.

Gérôme Melaet received his master degree (2006) and his Ph.D. degree (2011) from the Université Libre de Bruxelles (Belgium) under the guidance of Prof. Norbert Kruse. He received a FRIA doctoral grant from the Belgian Fund for Scientific Research (F.R.S.-FNRS) to conduct research on the design and performance of heterogeneous catalysts using conventional and nanotechnological preparation methods. In January 2012, Dr. Melaet joined Prof. Gabor Somorjai's group at the University of California at Berkeley (USA) as a post-doctoral fellow where he is in charge of the Fischer–Tropsch research project. He specializes in the characterization of heterogeneous catalysts under in situ conditions using advanced synchrotron X-ray spectroscopies available at the Advance Light Source of the Lawrence Berkeley National Laboratory, and has developed several in situ cells allowing catalysts to be studied under relevant conditions.

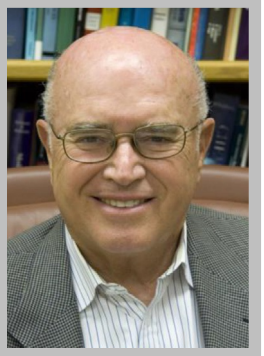

Gabor A. Somorjai studied Chemical Engineering at the Technical University in Budapest before emigrating to the United States in 1956, where was awarded his Ph.D. in Chemistry from the University of California (UC), Berkeley in 1960. He joined the IBM research staff until he was appointed Assistant Professor of Chemistry at UC Berkley in 1964 and was later promoted to Professor in 1972. Professor Somorjai has educated more than 130 Ph.D. students and 200 postdoctoral fellows. Professor Somorjai has received nearly every award in his field, among them the Honorary Fellowship of the Royal Society of Chemistry (2015), National Academy of Sciences Award in Chemical Sciences (2010), the 2010BBVA Foundation Frontiers of Knowledge Award, the Priestley Medal (2008), the National Medal of Science (2002), and the Wolf Prize (1998). He is the author of four textbooks and more than 1100 scientific papers in the fields of surface chemistry, heterogeneous catalysis, and solid state chemistry.

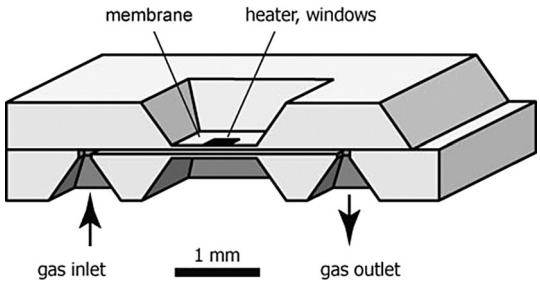

Figure 2. Sketch of TEM window sealed cell also called nanoreactor.

silicon wafers endowed with thin electron transparent membranes as windows. In theory, cells like this would allow the user to work at higher pressure, hence working to diminish the "pressure gap". However, this type of approach is still young, primarily due to the difficulties to produce and manipulate these cells. The high risk of leakage, as well as the rupture of the membrane due to pressure/temperature, is another drawback to the technique as it might seriously compromise the integrity of the TEM. Finally, the spatial resolution suffers as compared to E-TEM because it is now limited by the thickness of view windows and the gas flowing through the cell.

Despite these major drawbacks, the in situ cells have been successfully used and provided state of the art information to pinpoint structure-sensitive reactivity of surface sites. For example, the work of Vendelbo et al. shows the structural changes of Pt nanoparticles induced by CO.[25] Moreover, owing to the short time resolution of TEM, they were able to prove that the oscillatory behavior of the CO oxidation is synchronous with the periodic refacetting of the platinum nanoparticles. Zheng et al. also successfully used a commercial gas flow cell to study the oxidation of cobalt nanoparticles in real-time with a spatial resolution around 2 Å.[26] The authors evidenced the in situ evolution of the Kirkendall effect, the differential diffusion of multi-component alloys or oxides, occurring during the temperature-programmed oxidation of cobalt particles. Study of the nucleation and growth of Pt nanoparticles in liquid conditions using a window type cell were made possible, shedding light on the process of nanoparticles formation in a colloidal medium.[16,27]

Further information is needed to understand the impact of the electron beam on the matter and also on how much the dosing of the electrons can influence the in situ measurement.[24,28] Nevertheless, scanning TEM and TEM for in situ studies of gas–solid interaction is a robust tool which allows for atomic scale imaging under relevant conditions and thus provides complementary morphological and crystallographic evidence to information coming from the suite of other in situ imaging and spectroscopic techniques that average information over larger length scales.

In Situ Vibrational Spectroscopy

Elucidation of complex heterogeneous catalytic mechanisms at the molecular level is a challenging task, owing to the complexity of the structure of the catalyst surface.[29–31] Surface-sensitive and in situ techniques are required to probe the catalyst surfaces under working conditions. To that extend, some vibrational spectroscopic techniques such as infrared reflection absorption spectroscopy (IRAS),[32,33] polarization-modulation infrared reflection absorption spectroscopy (PM-IRAS),[34–37] and sum frequency generation vibrational spectroscopy (SFGVS),[38–40] offer surface-sensitivity and allow for real-time investigation.[34–40] In addition, these techniques also provide a comprehensive description of the surface functional groups existing on the working catalyst surfaces. Studies using IRAS and PM-IRAS performed in D. Wayne Goodman's research group, as well as other research groups have demonstrated their potential to study heterogeneous catalytic reactions at the solid–gas interface on model catalyst surfaces from ultra-high vacuum to near atmospheric pressures.

Several of these studies have examined the adsorption of molecules (e.g. CO, NO, O_2, H_2, CH_3OH) on monometallic and bimetallic transition metal surfaces (e.g. Pt, Pd, Rh, Ru, Au, Co, PdZn, AuPd, CuPt, etc.).[34,41–47] In spite of their usefulness in probing model planar surfaces, IRAS, and PM-IRAS techniques could not be applied to nanostructured catalysts because they are linear spectroscopic techniques. These techniques give surface information at the molecular level only when they are applied to well-defined planar model catalysts, such as a single crystal or an ultrathin film. Moreover, the absorption from the background gas or liquid phase will overwhelm the much smaller IR signal corresponding to the surface species at sub-monolayer coverage. Sum frequency generation vibrational spectroscopy is, however a second-order nonlinear optical process, which provides unique opportunities to probe surfaces and buried interfaces. SFG has been applied to problems in many disciplines of science and technology.[48–51] The use of SFG vibrational spectroscopy enables researchers to probe the reactions at the solid–gas, solid–liquid, and solid–solid interfaces. The technique renders possible the determination of chemical composition, orientation and arrangement of molecules, and reaction mechanisms on surfaces or buried interfaces. The basic operational principle of vibrational SFG technique relies on a second-order nonlinear optical process which involves the mixing of infrared (ω_{IR}) and visible light (ω_{VIS}) to produce light at the sum of two frequencies ($\omega_{SF}=\omega_{IR}+\omega_{VIS}$). Figure 3 shows an energy level diagram and optical transition for SFGVS, and also a schematic representation of the experimental setup for SFGVS. Two laser beams are spatially and temporally overlapped. To be SFG active, the vibrational mode of interest must be both IR and Raman active. Moreover, this process is forbidden in media with inversion symmetry under the electric-dipole (ED) approximation, but is allowed at surfaces or interfaces where the inversion symmetry is necessarily broken. Hence, it is highly surface specific unless additional electric field caused by the external source exists in the bulk. This means SFGVS can probe the adsorbates at the gas–solid or liquid-solid interfaces. A SFG spectrum can be obtained by monitoring the intensity of SFG output, while scanning the frequency of the IR light. SFG has contributed to the understanding of many surface-related phenomena on a truly molecular level.

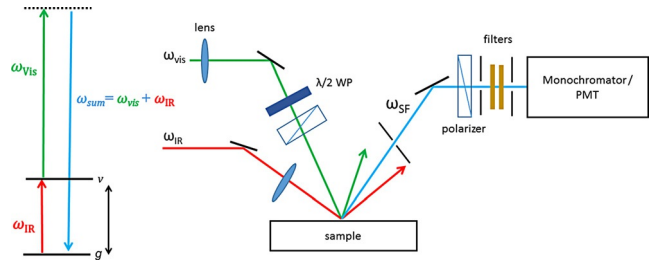

Figure 3. An energy level diagram and optical transition for SFGVS, and schematic of SFGVS system, which probe the vibrational signatures of adsorbed species on the surface.

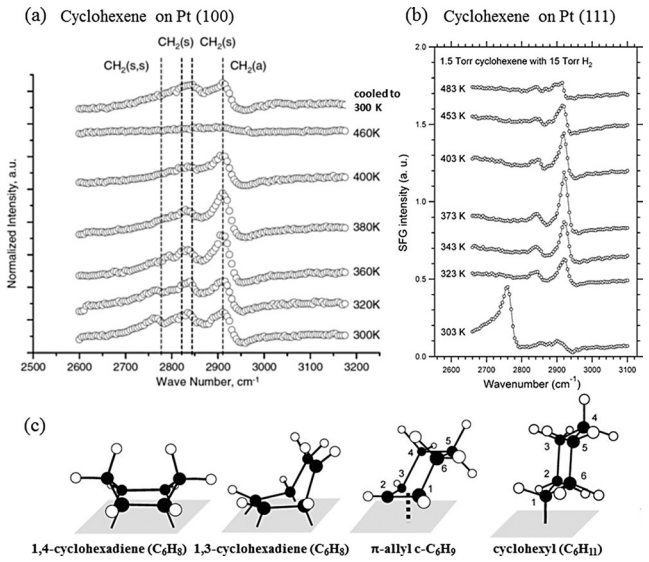

Figure 4. Temperature dependent SFG spectra of surface species under hydrogenation reaction of cyclohexene on a) Pt(100) [60] and b) Pt(111),[61] under 1.5 Torr of cyclohexene and 15 Torr of H_2. c) Schematic diagram of possible molecular structure of intermediates—1,4-cyclohexadiene (C_6H_8), 1,3-cyclohexadiene (C_6H_8), π-ally c-C_6H_9, cyclohexyl (C_6H_{11}).

Studies of solid–solid and solid–liquid interfaces have been growing in recent years, mainly attributed to the fact that no other vibrational spectroscopic techniques are capable of measuring molecular structure at interfaces.

As a nonlinear optical method, sum frequency generation vibrational spectroscopy offers in situ probing of molecular information under catalytic reaction conditions, such as orientation and composition. SFG is an excellent in situ technique that is able to bridge the gap between traditional surface science and applied catalysis. SFGVS has the detection sensitivity to probe surfaces with sub-monolayer coverage and to identify surface species during catalytic reactions. This way, SFGVS can provide direct evidence for reaction mechanism, and hence, reveals dynamic changes at a molecular level for the adsorbed molecules on catalyst surfaces. This was demonstrated on the Pt catalyzed hydrogenation of cyclohexene[52] and 1,3-butadiene.[53] Both reactions were found to be dependent on the size of catalyst, in what is a structure-sensitive reaction. This is because the strength of the metal–adsorbate bond is closely related to the coordination number of the surface metal atoms. Furthermore, surface morphology is determined by different surface sites such as terraces, steps, and kinks which are strongly correlated with surface coordination number. As a result, reaction rates are governed by both size and morphology.[54] To gain insight into structure-sensitive catalytic reactions at the molecular level, our group employed sum frequency vibrational spectroscopy to study catalytic hydrogenation of various hydrocarbons on well-prepared single crystals.[54–58] In the case of hydrogenation of cyclohexene on Pt(100) and Pt(111) single crystal surfaces,[59–61] it was found that cyclohexene hydrogenation is a structure sensitive reaction. Four surface intermediates are observed in the reaction pathways π-Ally c-C_6H_9, cyclohexyl (C_6H_{11}), 1,4-cyclohexadiene, and 1,3-cyclohexadiene (all shown in Figure 4c). The relative peak intensity of all species was found to be dependent on surface structure, temperature and partial pressure of hydrogen. Figure 4a and b show the temperature-dependent SFG spectra of surface species on Pt(100) and Pt(111) for hydrogenation of cyclohexene. On Pt(100), four major bands at 2780, 2805, 2865, and 2940 cm^{-1} are observed at 300 K. These peaks were assigned to 1,4-cyclohexadiene and π-allyl c-C_6H_9. An intensity drop at 2780 cm^{-1} was observed while increasing the surface temperature indicating the decrease of adsorbed 1,4-cyclohexadiene. On Pt(111), on the other hand at 303 K, a dominant band at 2760 cm^{-1} is observed and was assigned to 1,4-cyclohexadiene. At elevated temperatures, 1,3-cyclohexadiene and π-allyl c-C_6H_9 are identified from the vibrational band positions and their relative intensities, which are 2855, 2880, and 2900 cm^{-1} for 1,3-cyclohexadiene and 2840 and 2920 cm^{-1} for π-allyl c-C_6H_9, respectively.

Unlike cyclohexene hydrogenation, ethylene hydrogenation on Pt crystal surface is structure insensitive.[54] Two common surface-bound species are present in both Pt(111) and Pt(100) under reaction conditions—ethylidyne and di-σ-bonded ethylene. Although the concentrations of these two species are different, the reaction rates are essentially the same on the two Pt surfaces—these species act like spectators, and they do not participate in the catalytic ethylene hydrogenation. It was later determined that a third surface bound species, π-bonded ethylene, which is present at low concentrations on the Pt surfaces, turns over to ethane during the hydrogenation of ethylene.

Spectroscopic investigation under reaction conditions can also lead to an understanding of selectivity on crystal surfaces. This is crucial in developing processes that can achieve 100% selectivity of the desired product molecules, even out of many thermodynamically stable molecules in multipath reactions.[62–66] This goal is one of the major challenges in the field of catalysis and is colloquially known as "green chemistry". This research was exemplified in the multipath/multi-product hydrogenation of furan[67] and pyrrole.[58] The sum frequency generation vibrational spectroscopy was performed in situ to elucidate the product selectivity as a function of binding structure, temperature, and catalyst size. In the case of furan hydrogenation, the SFGVS data indicates that planar furan ring lies parallel to the metal surface under furan hydrogenation on Pt(100) and Pt(111) single crystal.[67] However, on the Pt(111), the reac-

tion product tetrahydrofuran (THF) is bound to the surface in an upright geometry, and another reaction product, butanol, is bound to the surface in a parallel orientation through its oxygen atom. Over Pt(100), both THF and butanol are bound to the surface in upright geometries. On both crystals, as temperature rises, the surface concentration of butanol increases. This was in agreement with the result observed with GC analysis. A temperature dependence on selectivity was observed during the hydrogenation of furan over Pt(111): THF was the dominant product at 90 °C while butanol was favored with 90% yield at 160 °C. In contrast, Pt(100) favored butanol production over THF at both 90 °C (>50%) and 160 °C (80%).

Another illustration[58] of the combination of the catalytic performances study with SFGVS spectra obtained in identical conditions is the study of adsorption and hydrogenation of pyrrole over Pt(111) and Rh(111) single crystal surfaces. Catalytic data indicated a difference in the selectivity for the two metals. SFGVS data reveals different adsorption geometries: pyrrole binds through the N atom to the Pt(111) surface in an upright geometry but binds to the Rh(111) surface through its aromatic π-electron with a slightly tilted geometry. According to the SFGVS results, the change of selectivity from Pt to Rh was explained by the orientation difference of the pyrrole on the surface over both catalyst surfaces at 298 K. Moreover, SFGVS results also provide evidence to the significant improvement of the turnover rates with the co-adsorbate 1-methylpyrrole. A blue shift in the wavenumber of N–H stretching modes was observed in the presence of 1-methylpyrrole. This suggests that 1-methylpyrrole interacts laterally with N-containing products. This interaction weakens the interaction of the N–H bond with the metal surfaces, reducing the desorption energy of the products. This allows pyrrolidine to desorb before continuing on to form the ring-opening product butylamine, which was found to be a reaction poison over both the Pt and Rh metal surfaces.

To bridge the "material gap" and obtain more information on the activity of a "real catalyst", one can use nanoparticles as model catalysts and like in the case of single crystal obtain molecular information about their interfaces with a liquid or a gas. Because of the surface-specific nature of SFG, one would naturally extend this technique to nanoparticles. Different from the single crystal surfaces, SFG signal appears in a broad solid angle depending on the size and shapes of the particles. Recently, Roke and co-workers have performed a series of theoretical and experimental studies to understand the use of SFG on small particles, and second-order nonlinear light scattering methods have been developed based on their work.[68,69] Two recent reviews have summarized their works.[70,71] Roke et al. first demonstrated SFG scattering from colloidal particles with broadband SFGVS Scheme on SiO_2 particles coated with stearic alcohol ($C_{18}H_{37}OH$) and dispersed in CCl_4.[72] The result suggests that the stearyl chains are strongly disordered on the particles. This is very different from the case of a closely packed stearic alcohol monolayer adsorbed on a planar silica surface.[73]

SFG is also employed to study reaction intermediates and catalytic selectivity on nanoparticle surfaces.[74,75] The use of ozone has proven to be an effective method for the removal/disordering of PVP from the surface of Pt[75] or Pd[76] nanoparticles without disturbing the particle size or shape, respectively. Some researchers demonstrated SFG measurements in total internal reflection (TIR) geometry,[74,77,78] shown in Figure 5(a),

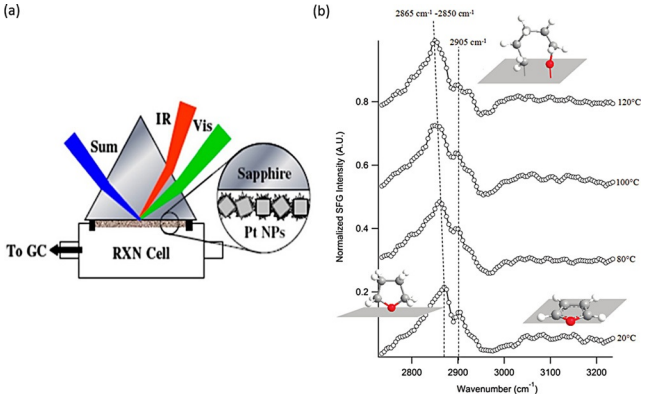

Figure 5. a) SFG vibrational spectroscopy at TIR configuration with a typical reaction cell used in our laboratory to study reactions on supported nanoparticles in real time.[74] b) Temperature-dependent SFGVS spectra acquired during furan hydrogenation (10 Torr of furan and 100 Torr of H_2) over 1 nm Pt nanoparticles.[67]

and show the advantage of eliminating the absorption attributed to bulk gas or liquid. TIR reduces the destructive interference associated with nonlinear optical process of small particle surfaces.[77,78] Therefore, this geometry allows for direct probing of solid–gas or solid–liquid interfaces, especially important for the complicated systems like nanoparticles under reactive atmospheres. For furan hydrogenation over colloidal Pt nanoparticles after removal of the organic capping agent, Figure 5(b) shows the SFG spectra of 1 nm Pt nanoparticles as a function of temperature. The SFG data indicates that THF has an upright geometry on the surface, the oxametallacycle intermediate is bound to the surface during the reaction, and the surface species is not temperature sensitive.[67] SFGVS data show nanoparticles catalysts all exhibit similar surface bound reaction intermediates—THF and oxametallacycle—yet the propylene product is absent from the spectrum. On the other hand, the SFGVS data on single crystals [both (111) and (100)] indicate that the surface species are THF and butanol. The difference in intermediates agrees with the difference in production distribution (i.e. selectivity) as indicated by catalytic testing. Briefly, the nanoparticles show greater selectivity toward propylene, butanol and ring cracking products. In the case of ethylene hydrogenation, SFGVS on Pt nanoparticles showed the existence of ethylidyne and di-σ-bonded species, indicating the similarity between single-crystal and NP systems.[74]

In a recent study, the SFG study of crotonaldehyde hydrogenation on Pt/TiO_2 and Pt/SiO_2 catalyst showed the selective amplification of C=O bond hydrogenation on Pt/TiO_2.[79] Coupling gas-phase catalytic reactions with SFGVS reveals how the interaction between the metal nanoparticles and their support can control catalytic performance. SFG spectra obtained for Pt/TiO_2 catalyst indicate the presence of a crotyl-oxy surface intermediate. This result identified a unique reaction pathway for

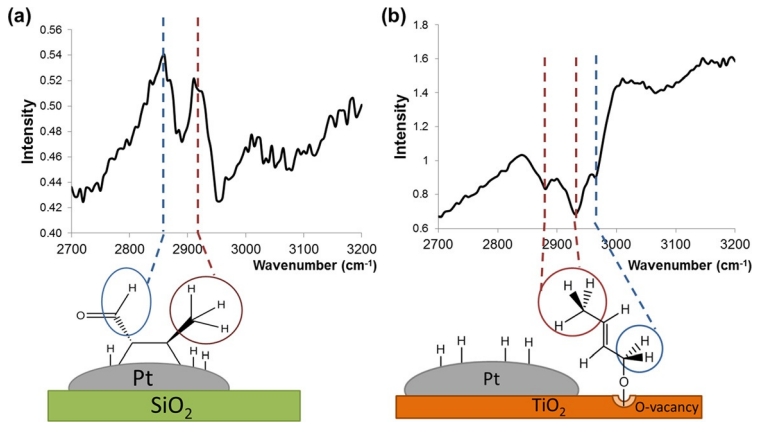

Figure 6. SFG spectra for a) Pt/SiO_2 and b) Pt/TiO_2 under reaction conditions of 1 Torr crotonaldehyde, 100 Torr hydrogen, and 669 Torr argon at 120 °C.[79]

Pt/TiO_2, which selectively produces alcohol products. The interpretation of spectroscopic data (Figure 6) shows that in the adsorption through the aldehyde oxygen atom to an O-vacancy site on the TiO_2 surface, the C=O bond of crotonaldehyde is activated, for hydrogenation. On the other hand, the catalytic and spectroscopic data obtained for the Pt/SiO_2 catalyst shows that SiO_2 has no active role in this reaction. This work showed that crotyl-oxy bonding at defect sites promotes hydrogenation of the carbonyl group rather than the unsaturated group. This is the first spectroscopic observation that oxygen vacancies on the TiO_2 surface served as the site for the selective hydrogenation of the aldehyde group.

Overall, these examples demonstrate that SFGVS has been a powerful tool to provide information about reaction pathways, intermediates, and structure selectivity on single-crystal and nanoparticle surfaces under reaction conditions.

Ambient Pressure X-ray Photoelectron Spectroscopy

X-ray Photoelectron spectroscopy has conventionally been an ultrahigh-vacuum technique because of the small mean-free path of the photoelectron emitted. From the late 60s through the 80s,[80–87] "high pressure" XPS developed continuously, but slowly. It was with the advent of third-generation synchrotron radiation sources that ambient pressure X-ray photoelectron spectroscopy experienced its main breakthrough with pioneering groups at the Advanced Light Source (ALS) in Berkeley.[88–90]

In fact, much like the E-TEM with an E-cell described earlier, these AP-XPS pioneers used of a series of differential pumping stages and electron lenses before the analyzer, and a metal cone with a narrow orifice in front of the sample which allows for operation at high pressures (see Figure 7). Other than a few improvements regarding the control of the electron path in the multiple differential pumping stages, the third-generation of AP-XPS analyzers in use today are relatively similar to the first generation developed by Ogletree, Salmeron, and Bluhm.

In practice, laboratory XPS using conventional X-ray sources (Al and Mg K) are functional yet the high brightness and tunable energy of the X-rays from synchrotron radiation makes synchrotron-based AP-XPS more attractive and more versatile in their use than laboratory AP-XPS, which are now commercially available. This is particularly attractive in the study of heterogeneous catalysis as the elemental composition and redox states of the surface and subsurface region can be evaluated under catalytically relevant conditions.

An illustrative example of the use of AP-XPS over model catalyst is the study of bimetallic nanoparticles of Pt-Rh and Pd-Pt and their reconstruction under different reaction conditions (oxidative versus reductive atmosphere).[91] This work, as well as many others since published, evidences the importance of tunable synchrotron X-rays to determine a true picture of the active catalyst phase. In fact, Tao et al.[92] also demonstrated the reversible surface restructuration of Pd-Rh bimetallic particles (50-50 composition) under alternating oxidative and reductive atmospheres. The incident photon energy was chosen such that the inelastic mean free path of the photoelectrons gave a probing depth of 7 to 16 Å. The experiments showed, starting with Rh-rich surfaces in vacuum, that the particles do not change in NO atmosphere yet palladium segregated to the surface of the particle when CO is introduced. Many other works on binary or bimetallic systems over the years have demonstrated the importance of in situ characterization and especially the use of near ambient pressure X-ray photoelectron spectroscopy.[17,92–96]

Bimetallic systems are not the only interesting system to be studied using synchrotron radiation source. In fact, a great deal of information on the oxidation states of monometallic systems or the influence of the oxide supports can be obtained via AP-XPS. Rh nanoparticles were studied in the size range of 2–11 nm for the lean-burn oxidation of carbon monoxide.[97] The catalytic data evidenced a 7-fold increase in the activity of 2 nm particles when compared to 7 nm particles. AP-XPS demonstrated that 2 nm particles were substantially oxidized, while 7 nm particles stayed mostly metallic under the same reaction conditions (O_2-rich conditions). A similar work was done on the CO oxidation over Ru nanoparticles by Park et al.[93] and showed a different catalytic behavior with a higher turnover rate for larger particles. Yet they also found that

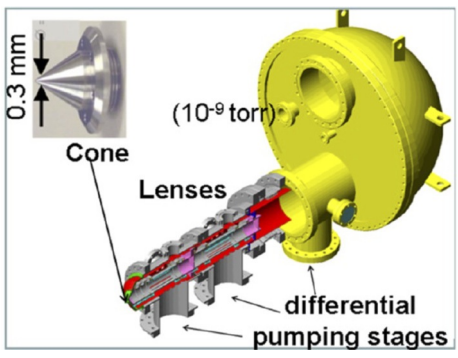

Figure 7. Analyzer from ambient pressure X-ray photoelectron spectroscopy, the insert shows the metal cone facing the sample.

smaller nanoparticles oxidized easier than larger particles when exposed to identical reaction conditions.

More recently AP-XPS aided in the understanding of the Pt-assisted reduction of ceria.[98] Briefly, the authors demonstrated that the presence of Pt on ceria promoted the reduction of Ce^{4+} to Ce^{3+} under H_2 atmosphere (100 mTorr).

Tunable X-ray photoelectron spectroscopy was also successfully used to demonstrate the importance of the strong metal–support interaction (SMSI).[99] When submitted to different conditions, it was demonstrated that size-controlled cobalt nanoparticles can either wet TiO_2 support or inversely can be encapsulated by the support. In practice, the authors evaluated the atomic percentage of Co at the surface of the catalyst from the Co 2p core level XPS spectra under different conditions. The percentage of surface Co ($\%Co_{surface}$) was found to increase from 25% (O_2 at 350 °C) to 35% under H_2 at 250 °C. Conversely, when the catalyst is reduced to 450 °C, the $\%Co_{surface}$ drops to 20%.

Finally, Graciani et al. have used AP-XPS to show the importance of metal–metal oxide interface in the hydrogenation of CO_2.[100] When studying the interaction of CO_2 with ceria and/or copper, the authors evidence the presence of strongly absorbed carbonate on pure ceria(111) whereas Cu(111) alone did not show any sign of CO_2 adsorption. In their paper, the authors successfully evidenced the presence of a carboxylate when ceria is deposited on Cu(111). Based on their results, obtained both with AP-XPS and Infrared Reflection-Absorption Spectroscopy (IRAS) measurements, the authors concluded that the formation of methanol is favored on the CeO_x/Cu(111) interface because of the existence of this carboxylate intermediates ($CO_2^{\delta-}$).

These different examples are to demonstrate the usefulness of AP-XPS in the field of surface science in general and catalysis in particular. It is a precious tool for those who want to access information regarding the chemical composition of a surface under reaction conditions. Yet, one might argue that much like the E-TEM the pressure gap is still an issue, and even if constant efforts are made to overcome it, we ought to consider it to be the major drawback of this technique, along with the lack of spatial resolution. Currently, we believe that the future of AP-XPS resides in the use of window cells similar to those currently developed for environmental TEM. Another drawback to this technique would be the lack of spatial and time resolution.

X-ray Absorption Spectroscopy

Synchrotron-based X-ray absorption spectroscopy (XAS) also provides a mean to study the heterogeneous catalysts under reaction conditions at high temperature and above atmospheric pressures.[101] XAS spectrum can be divided in two components: Extended X-ray absorption fine structure (EXAFS) and near-edge X-ray absorption fine structure (NEXAFS), both of which provide complimentary information of a catalyst at work. Both spectroscopic techniques are based on the energy dependence of the photoabsorption, yet each component provides its own unique information. The "near-edge" part of the spectrum as well as the adsorption edge itself informs about the chemical state environment such as the oxidation state, symmetry or the local charge distribution. The extended region, on the other hand, allows gathering information on the local environment of the atoms absorbing the incident photons such that the coordination number as well as the distance with the neighboring atoms can be resolved.

NEXAFS measurements can easily be done using soft X-ray (400–3000 eV) to investigate the oxidation state of the first and second row of transition metals (L-edge). The use of soft X-ray instead of more energetic photons presents both pros and cons: the low energy photons have a small penetration depth, yet they are easily adsorbed by gaseous molecules. On the other hand, hard X-rays (i.e. 5 to 20 keV) do not suffer from gaseous absorption which makes them particularly suitable for in situ measurements. However the penetration depth is a few orders of magnitude larger than for soft X-rays. Nevertheless, a surface sensitive measurement can be achieved in both cases, as we will demonstrate later.

The surface sensitivity of NEXAFS and EXAFS can be tuned either by the means used to measure the absorption spectra or a careful selection of samples. Indirect measurement of the X-ray absorption, in opposition with the measurement by transmission, can be sometimes advantageous: impact on the depth into the sample probed and the ability to record measurement in situ. The indirect measurement is based on the measurement of the emission of X-ray fluorescence or electrons (Auger and secondary scattering electrons).[102,103] The collection of X-ray fluorescence is bulk measurement as the produced photons are weakly absorbed and can escape from the bulk of the material. This mode of collection has the advantage of being able to be collected through high pressure or a liquid phase. It is worth noticing that fluorescence yield can be used as a surface measurement for small and ultra-small particles where the bulk to surface ratio approaches one. On the other hand, monitoring XAS using a total electron yield (TEY) mode is fairly sensitive to the surface since the escape depth of the electrons collected is below 3 nm. In practice, TEY is measured using a picoammeter to monitor the compensating current flowing between the sample and ground.

Traditionally, EXAFS have been applied more extensively for in situ characterization than NEXAFS because of the lesser limitation of higher energy X-rays. Nuzzo's work on bimetallic particles is a good illustration of in situ EXAFS capabilities. In an early publication,[104] Pt-Ru nanoparticles supported on carbon black were prepared via the reduction of $PtRu_5C(CO)_{16}$. EXAFS indicates the formation of bimetallic nanoparticles with non-statistical distribution of the metal atoms. Moreover, the authors demonstrated that Pt preferentially occupy surface sites and that, upon reversible oxidation, the particles are formed of an oxide shell with a metal core. Those results are confirmed in a subsequent work where the support is varied.[105]

Liu et al. have investigated the electronic structure of cobalt nanocrystals in a liquid suspension using XAS at the Co L-edges. The results evidenced that Co particles interact stronger with solvent molecules in the initial stages of nucleation and growth, while the interaction with the surfactant/capping

agent is favored at later stages.[106] In the same vein, Alayoglu et al. studied bimetallic Pt-Ru alloy and core-shell structures produced by a colloidal method.[107] They evidenced the different behavior of these two structures when exposed to identical atmospheres. This work provides a unique example of structure–activity relationship. Using an in situ gas flow cell, Zheng et al. have studied the structure of cobalt and bimetallic Co-Pt in oxidative and reductive environments.[108] The study shows that the presence of Pt in the bimetallic particles helps reducing Co at lower temperature than of the pure cobalt particles. In fact, cobalt is reduced at 38 °C for the Co-Pt, whereas Co L_3-edge does not show any sign of reduction until 250 °C in the case of Co particles (Figure 8).

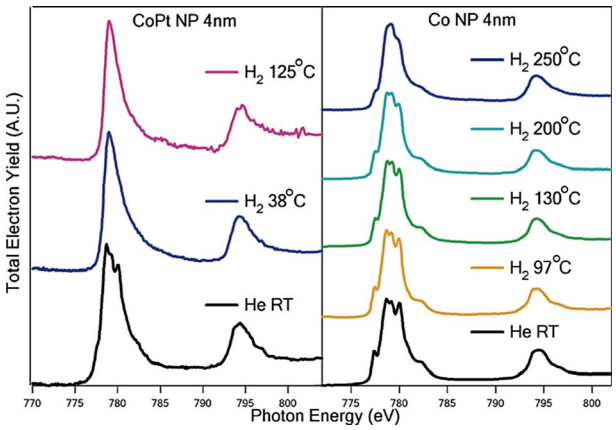

Figure 8. Cobalt L-edge spectra to compared the reducibility of bimetallic cobalt platinum nanoparticles (left) and monometallic cobalt nanoparticles (right) under reaction conditions in pure hydrogen.[108]

The same year, Föttinger et al. used in situ XAS to investigated palladium zirconia catalysts at work.[109] Briefly, the work demonstrated the formation of PdZn alloy upon methanol steam reforming reaction conditions. Exposing the catalyst to oxygen at 350 °C lead to the segregation of PdZn into metallic palladium and zirconia proving that the alloying is reversible.

A recent work by Nuzzo et al. compared the behavior of SiO_2-supported Pt and SiO_2-supported Pd nanoparticles in the hydrogenation of ethylene.[110] The study showed that palladium nanoparticles irreversibly sinter to form larger particles due to the gaseous environment (i.e. more pronounced in ethylene rich environment). On the other hand, platinum nanoparticles do not sinter, as it is the case for palladium. Instead, the exposure to ethylene-rich conditions leads to a profound change in the chemical composition of Pt with the appearance of two additional bonding contributions attributed to ethylidyne absorbed at the surface and Pt–C species on and in the particles. Finally, once H_2-rich conditions are restored, the authors noticed the disappearance of the ethylidyne contribution but not that of Pt–C. This work is, to our understanding, a good example of the importance of in situ characterization to investigate the dynamic structural complexity of catalysts as its environment is affecting the active phase. To this end, in the last decade, continuous efforts have been made to provide time-resolved XAS in situ measurements and thus monitor the changes in composition and structure as the catalyst is exposed to reaction conditions. A few examples are given hereafter as an indication.

Time-resolved EXAFS studies by Imai et al. monitor the formation of platinum oxide in acidic aqueous solution under positive overpotential with a time resolution of 0.9 s.[111] Briefly, using hard X-ray and energy dispersive X-ray absorption spectroscopy the authors demonstrate the gradual formation of a surface platinum oxide through the formation and shortening of the Pt–O bonds. Ferri et al. used modulation excitation X-ray absorption spectroscopy (MSE) to probe Pd/Al_2O_3 and Pt/Al_2O_3 for the NO reduction by CO and CO oxidation, respectively. MSE is based on pulse or fast transients studies of a catalysts while monitoring the changes by spectroscopy (time resolution = 0.26 s). The use of non-steady state conditions, such as this one or others like steady state isotopic transient kinetics analysis (SSITKA)[112–114] and chemical transient kinetics (CTK),[115–117] are especially suited to obtain information on the actives species and mechanistic clues. Using this method the authors revealed the evolution of the surface species and the surface composition of the catalysts.

A final example of the use of time-resolved XAS is the work by Gaskell et al. on the crotyl alcohol selective oxidation over supported palladium nanoparticles produced by incipient wetness impregnation.[118] Using an in situ transmission cell, the authors monitored the PdO content of Pd nanoparticles with a time resolution of 0.75 s. They showed that the selective oxidation of the crotyl alcohol is regulated by the redox properties of the particles (oxidation-reduction cycle). In practice, the authors found a nonlinear, inverse correlation between the redox capacity of the nanoparticles and the catalytic oxidation of the reactant. In other words, crotyl alcohol conversion requires the presence of palladium oxide yet the selectivity to crotonaldehyde was determined by the ease of reducibility of the PdO. However, if the reducibility is too high, the particles are readily reduced to metallic palladium and the reaction is changed to the decarbonylation of crotyl alcohol to CO and propane.

Future of In Situ Measurements

In these sections, we highlight advances made in SFG spectroscopy, and X-ray- and electron-based techniques that combine electronic spectroscopy with high spatial or temporal resolution. STXM technique has already found applications in catalytic reaction studies both in situ and ex situ. Ptychography and XPCS, yet in their infancy for dynamic systems, have potentials to revolutionize the field.

Technical development of sum frequency generation spectroscopy

SFG spectroscopy technique has been used successfully to probe surfaces and interfaces of a wide range of materials in various disciplines. Recently, SFGVS has enjoyed a rapid growth as more laboratories around the world have adopted the tech-

nique. It also has made significant progress on the technological development and application of catalysis. An important technical advancement is the development of broadband sum frequency vibrational spectroscopy (so-called broadband SFGVS or BB-SFGVS). It is gaining popularity in recent years owing to significant improvements in the speed and sensitivity of charge coupled device detectors (CCD).[119] Different from the conventional approach to an SFGVS experiment which scans the IR frequency of a picosecond (or nanosecond) pulse laser, BB-SFGVS makes use of the broad bandwidth of a femtosecond (fs) IR laser pulse and allows for multiplex detection of SFG spectra using a CCD detector. BB-SFGVS generates an entire SFG spectrum over a broad range of wavenumbers and can be obtained with short acquisition times and without wavelength tuning. The spectrum width in the vibrational wavenumber region is defined by the width of IR pulse, typically 200 cm^{-1} with a 100 fs pulse duration, and the spectrum resolution is determined by the spectral width of the visible beam, typically limited to 10–20 cm^{-1}. BB-SFGVS has been demonstrated to have the ability to obtain good quality spectra with sufficient spectral resolution and a high signal-to-noise ratio as well as the advantage of performing ultrafast dynamic studies.[120–123] For example, Roeterdink et al. investigated the model CO oxidation reaction on the Pt(111) surface by in situ monitoring of reaction kinetics using broadband SFGVS as a function of surface temperature. Kinetic parameters of the CO oxidation reaction over Pt(111) were obtained as a result of this work.[123] Kutz et al., studied reaction pathways of ethanol electrooxidation on polycrystalline platinum catalysts in acidic electrolytes.[122] Very recently, Wang's group at the Pacific Northwest National Laboratory developed a novel approach to advance BB-SFGVS to have high resolution capability.[124] The emergence of high-resolution broadband sum-frequency generation vibrational spectroscopy (HR-BB-SFGVS) with sub-wavenumber resolution offers new opportunities for obtaining and understanding the spectral lineshapes and temporal effects in SFGVS. Particularly, the high accuracy of the HR-BB-SFGVS experimental lineshape provides detailed information on the complex coherent vibrational dynamics through direct spectral measurements.[124] This sophisticated system would have the potential to study complex catalytic networks to identify surface species and intermediates with high temporal resolution. With the advent of femtosecond coherent light sources, time-resolved BB-SFGVS technique emerged to study ultrafast surface dynamics.[125,126] They can characterize the structure and dynamics of surface species directly. Nagao et al. reported ultrafast vibrational energy transfer in the layers of D_2O and CO on Pt(111) under ultrahigh vacuum condition.[125] They observed transient spectral changes in the CO and OD stretching regions by introducing 150 fs pump pulses at 400 nm to excite electrons in the metal to create hot electrons. They concluded that this phenomenon is attributed to the coupling of hot electrons with the frustrated motions of CO adsorbates and the interaction of CO with co-adsorbed D_2O on Pt. Because numerous important catalytic reactions depend on high frequency dynamic processes such as fast energy transfer and electron transfer, we believe that time-resolved SFGVS will play an important role in understanding the charged nature of catalytic reactions at surfaces or interfaces.

Another important technical development is sum frequency generation vibrational spectro-microscopy (SFGVSM).[127–129] It provides the unique advantage of combining microscopy and spectroscopy into one surface-sensitive technique. With the advantage of IR input, labeling of the molecule is not required because molecules can be identified through their vibrational resonances and fingerprints. Although SFG microscopy as a nonlinear optical method is more complex in terms of instrumentation than conventional fluorescence microscopy, it allows the optical imaging of molecules at interfaces with chemical contrast. This method has become an important tool for obtaining spatial information about the biological samples, such as cellulous[130] and collagen fibers,[131] specifically for cellular biology at both the surface and interface.[132,133] The SFGVS microscopy was first set up by Flörsheimer et al.,[129] they observed an SF image of a Langmuir–Blodgett (LB) monolayer of arachidic acid with the IR frequency tuned into the resonant symmetric and asymmetric CH_3 stretching frequencies. However, the image is distorted because the SFG output is at an oblique angel with their setup. By using a diffraction grating to avoid that problem, Baldelli et al. have used the SFGVS microscopy to study a series of self-assembled monolayers on various substrates.[128,134,135] They were able to obtain a spatial resolution close to 1 μm, which is much higher than what can be obtained in conventional IR microscopy. In applying this to a catalytic surface, Cimatu and Baldelli used SFGVS microscopy on a Pt surface.[136] An inhomogeneous local distribution of CO on Pt (shown in Figure 9) was revealed by SFG imaging indicat-

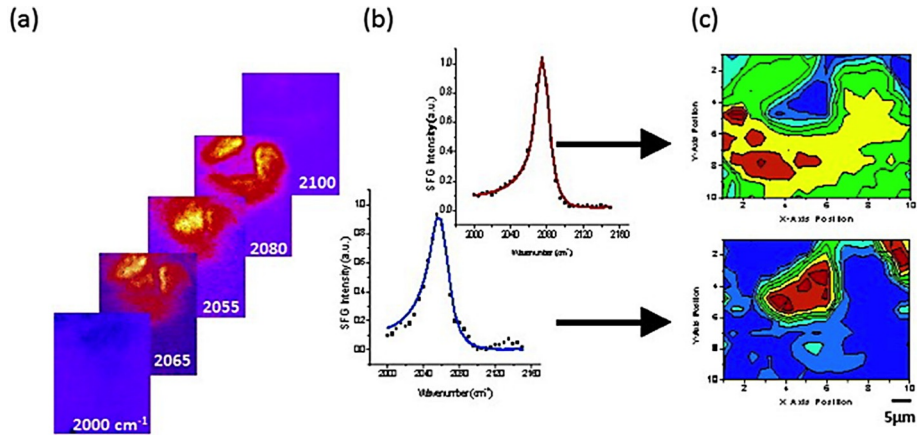

Figure 9. a) Unprocessed SFG image of CO on platinum obtained at various IR wavenumbers. b) Spectra are extracted from the images obtained at each wavenumber interval c) SFG image maps of the spatial distribution of CO on a Pt surface.[136]

ing a heterogeneous Pt surface, presumably for several reasons, such as dipole-dipole coupling, defects, and surface coverage. With the ability to visualize the surface, they demonstrated the importance of surface inhomogeneity which contributed significantly to our understanding of such catalytic systems. The spatial resolution of SFGVS microscopy can be further improved to 0.6 μm by focusing both IR and visible light at collinear-geometry.[132]

Scanning transmission X-ray microscopy

STXM offers chemical sensitivity and speciation of X-ray spectroscopy and spatial resolutions well below 50 nm, hence compliments to electron microscopy and the spectroscopic techniques equipped within. In STXM, synchrotron X-rays are focused to 10 s of nanometers in the near field using diffraction plates (i.e. Fresnel zone plates), and X-ray transmission through thin samples are measured across the absorption edges of elements of interest by scanning along the sample plane. By this way, chemical fluctuations in the nanometer scale could be mapped with high spatial resolutions for low *z* elements (C, O, N, F, Mg, Al, Si, P, Cl, etc.), transition metals and lanthanides, which usually constitute the active and dynamic components of a catalyst.

Gas phase molecules, at absorption lengths in the order of millimeters and ambient pressures, have negligible X-ray cross-sections in the soft X-ray regime, and allow STXM imaging under reactive gas atmospheres. This was demonstrated for a Fe-based Fischer Tropsch catalyst in 1 atm of H_2+CO (2:1) reaction. Sub-micron sized catalyst grains of FeO_x supported on SiO_2 were mapped at the Fe L and O K absorption edges during CO hydrogenation.[137] This study revealed for the first time chemically dynamic Fe/FeO catalyst under working conditions of an industrially-relevant catalytic process.

STXM could, in principle, be employed to measure adsorption transients of carbon at sub-monolayer coverage for high surface area catalysts, supports and membranes. Therefore, kinetics of surface adlayer formation could be determined. It should be noted that the use of resonant and non-resonant photon energies allows chemically specific spatio-temporal distribution of various different heteroatom adsorbates to be monitored. By this way, for example, catalytic site heterogeneity for zeolites could be visualized in relation to various acid (or base) site types (Brønsted vs. Lewis) or strengths (weak, medium, or strong).[138,139] As a future challenge, molecular recognition for gas separation membranes like metal–organic frameworks (MOFs) can be studied in terms of metal–adsorbate bonding using STXM in situ.

Mesoscale catalyst supports and matrices are ideal systems to study changes in chemical composition and distribution in the single particle level using STXM. Soft materials such as enzymes and polymeric membranes (e.g. Nafion and somehow MOFs), however, still remain a challenge for STXM and coherent beam techniques. Because high flux and dosage of X-rays could be detrimental for structural and chemical integrity of organic substances, while inorganic matter should be more resistive to radiation damage.

X-ray and electron ptychography

Typical catalyst particles are only a few nanometers, and can be studied at single particle level using ptychography. In Ptychography, STXM images are measured at multiple and overlapping diffraction spots in the sample plane. The ptychographs are thus obtained from these STXM images via specific and dedicated program using a phase retrieval algorithm.[140] Phase information can be retrieved from reconstruction of diffraction intensities.[141] By this way, ptychography provides magnitude and phase information of X-rays (or electrons) interacting with matter (e.g. catalysts). A record spatial resolution of 3 nm was reported using soft X-rays and a 60 nm zone plate. This was demonstrated for an iron olivine-based Li-ion battery cathode in the partially delithiated state,[142] and illustrated potentials of using of ptychography in energy sciences, and possibly in catalysis field. Furthermore, ptychographic reconstruction substitutes magnetic lenses in electron microscopy for obtaining high spatial resolution.[141] This aspect of the technique is essential in studying magnetic materials such as Fe, Co, Ni, and their alloys, which often utilized as catalyst particles.

X-ray photon correlation spectroscopy

XPCS uses resonant far field scattering of highly coherent X-rays,[140] and provides high chemical sensitivity and temporal resolution. Time transients at nanosecond time delays could in principle be obtained with elemental speciation. This renders possible investigation of far-from-equilibrium conditions and initial stages of chemical and catalytic transformations. Slow dynamical processes in the order of seconds such as Brownian motion of Au nanoparticle colloids[143] or diffusion constant of Pd nanoparticle colloids[144] in glycerol were reported via XPCS using second generation synchrotron facilities. Faster timescales could be realized with the advent of brighter radiation sources with diffraction limited beams.

For soft X-rays, photon wavelengths measure in the 10 s of Angstroms, larger than dimensions of typical interatomic distances and unit cells, yet in the same order of magnitude as micropores in zeolites and MOFs and mesopores of mesoscale materials. Hence, non-equilibrium dynamic fluctuations induced by adsorbed gas molecules or upon reaction and surface diffusion could be studied using XPCS. This aspect of XPCS is reminiscent of the small angle scattering techniques, with the exception that XPCS evaluates dynamic structure factor in the time domain. This is the real strength and promise of XPCS towards catalysis, where high frequency structural and chemical variations are targeted to capture reaction kinetics. This is especially attractive to probe porous materials, which are common to both catalysts and membranes, under realistic conditions as gas molecules condense on surfaces and alters morphology and chemistry of confined volumes. Recent advances in detector technologies (charge-coupled devices, complementary metal-oxide sensors, etc.)[145–149] and future advent of brighter synchrotron sources will bring coherent X-ray tech-

niques like XPCS closer to the service of colloidal, surface and interface sciences, and in situ/in operando studies.

General Conclusions

The use of in situ characterization techniques in heterogeneous catalysis has helped to identify previously unknown surface phenomena. The reversibility of many of these changes and the dynamic adaptation of surfaces to new environments highlights the importance of surface analysis under actual reaction conditions and the perpetual need to improve characterization techniques.

As a final comment, on the subject, we would like to point out that spatial resolution must be pushed forward. All of the spectroscopic methods presented in this Review are ensemble-average measurements. However, catalytic materials display heterogeneities in terms of composition, structure, and thus reactivity of active sites depending on their position within the material. A high spatial resolution, such as the one already achieved in TEM, would allow for a direct correlation between structure and composition. Moreover, as indicated by the time-dependent experiments described, we know that the catalysts also change with time (change in reactant coverage, change of structure, composition, etc.). The combination of "ultra-fast" spectroscopy at the particle level should provide useful information on the relationships between structure and catalytic performances (activity and selectivity).

Acknowledgments

The work shown in this review article was supported by the Director, Office of Science, Office of Basic Energy Sciences, Division of Materials Sciences and Engineering of the US Department of Energy under Contract No. DE-AC02-05cH11231.

Keywords: EXAFS · in situ measurement · nanoreactors · synchrotron-based techniques · TEM · XPS

[1] E. D. Boyes, P. L. Gai, *Ultramicroscopy* **1997**, *67*, 219.
[2] R. Sharma, K. Weiss, *Microsc. Res. Tech.* **1998**, *42*, 270.
[3] T. W. Hansen, J. B. Wagner, *Microsc. Microanal.* **2012**, *18*, 684.
[4] P. L. Hansen, J. B. Wagner, S. Helveg, J. R. Rostrup-Nielsen, B. S. Clausen, H. Topsøe, *Science* **2002**, *295*, 2053.
[5] H. Yoshida, S. Takeda, T. Uchiyama, H. Kohno, Y. Homma, *Nano. Lett.* **2008**, *8*, 2082.
[6] A. R. Harutyunyan, G. Chen, T. M. Paronyan, E. M. Pigos, O. A. Kuznetsov, K. Hewaparakrama, S. M. Kim, D. Zakharov, E. A. Stach, G. U. Sumanasekera, *Science* **2009**, *326*, 116.
[7] S. M. Kim, C. L. Pint, P. B. Amama, R. H. Hauge, B. Maruyama, E. A. Stach, *J. Mater. Res.* **2010**, *25*, 1875.
[8] R. Sharma, S. W. Chee, A. Herzing, R. Miranda, P. Rez, *Nano Lett.* **2011**, *11*, 2464.
[9] M. He, B. Liu, A. I. Chernov, E. D. Obraztsova, I. Kauppi, H. Jiang, I. Anoshkin, F. Cavalca, T. W. Hansen, J. B. Wagner, *Chem. Mater.* **2012**, *24*, 1796.
[10] S. Helveg, C. López-Cartes, J. Sehested, P. L. Hansen, B. S. Clausen, J. R. Rostrup-Nielsen, F. Abild-Pedersen, J. K. Nørskov, *Nature* **2004**, *427*, 426.
[11] M. R. Ward, E. D. Boyes, P. L. Gai, *ChemCatChem* **2013**, *5*, 2655.
[12] Z. Peng, F. Somodi, S. Helveg, C. Kisielowski, P. Specht, A. T. Bell, *J. Catal.* **2012**, *286*, 22.
[13] H. Yoshida, Y. Kuwauchi, J. R. Jinschek, K. Sun, S. Tanaka, M. Kohyama, S. Shimada, M. Haruta, S. Takeda, *Science* **2012**, *335*, 317.
[14] Y. Kuwauchi, S. Takeda, H. Yoshida, K. Sun, M. Haruta, H. Kohno, *Nano Lett.* **2013**, *13*, 3073.
[15] E. A. Stach, P. J. Pauzauskie, T. Kuykendall, J. Goldberger, R. He, P. Yang, *Nano. Lett.* **2003**, *3*, 867.
[16] H. Zheng, R. K. Smith, Y. W. Jun, C. Kisielowski, U. Dahmen, A. P. Alivisatos, *Science* **2009**, *324*, 1309.
[17] S. Alayoglu, S. K. Beaumont, F. Zheng, V. V. Pushkarev, H. Zheng, V. Iablokov, Z. Liu, J. Guo, N. Kruse, G. A. Somorjai, *Top. Catal.* **2011**, *54*, 778.
[18] H. L. Xin, S. Alayoglu, R. Tao, A. Genc, C. M. Wang, L. Kovarik, E. A. Stach, L. W. Wang, M. Salmeron, G. A. Somorjai, H. Zheng, *Nano Lett.* **2014**, *14*, 3203.
[19] S. Helveg, C. F. Kisielowski, J. R. Jinschek, P. Specht, G. Yuan, H. Frei, *Micron* **2015**, *68*, 176.
[20] R. Agarwal, D. N. Zakharov, N. M. Krook, W. Liu, J. S. Berger, E. A. Stach, R. Agarwal, *Nano Lett.* **2015**, *15*, 3303.
[21] S. B. Simonsen, I. Chorkendorff, S. Dahl, M. Skoglundh, J. Sehested, S. Helveg, *J. Am. Chem. Soc.* **2010**, *132*, 7968.
[22] S. B. Simonsen, I. Chorkendorff, S. Dahl, M. Skoglundh, J. Sehested, S. Helveg, *J. Catal.* **2011**, *281*, 147.
[23] F. Behafarid, S. Pandey, R. E. Diaz, E. A. Stach, B. R. Cuenya, *Phys. Chem. Chem. Phys.* **2014**, *16*, 18176.
[24] Y. Liu, Y. Sun, *Microsc. Microanal.* **2014**, *20*, 1636.
[25] S. B. Vendelbo, C. F. Elkjær, H. Falsig, I. Puspitasari, P. Dona, L. Mele, B. Morana, B. J. Nelissen, R. van Rijn, J. F. Creemer, *Nat. Mater.* **2014**, *13*, 884.
[26] H. L. Xin, K. Niu, D. H. Alsem, H. Zheng, *Microsc. Microanal.* **2013**, *19*, 1558.
[27] C. B. Murray, *Science* **2009**, *324*, 1276.
[28] D. Bufford, S. H. Pratt, T. J. Boyle, K. Hattar, *Chem. Commun.* **2014**, *50*, 7593.
[29] J. W. Niemantsverdriet, *Spectroscopy in catalysis*, Wiley, **2007**.
[30] G. Rupprechter, *Catal. Today* **2007**, *126*, 3.
[31] A. J. Foster, R. F. Lobo, *Chem. Soc. Rev.* **2010**, *39*, 4783.
[32] M. Chen, D. Kumar, C. W. Yi, D. W. Goodman, *Science* **2005**, *310*, 291.
[33] M. J. Lundwall, S. M. McClure, D. W. Goodman, *J. Phys. Chem. C* **2010**, *114*, 7904.
[34] E. Ozensoy, D. C. Meier, D. W. Goodman, *J. Phys. Chem. B* **2002**, *106*, 9367.
[35] M. Borasio, O. Rodríguez de La Fuente, G. Rupprechter, H. J. Freund, *J. Phys. Chem. B* **2005**, *109*, 17791.
[36] C. Weilach, S. M. Kozlov, H. H. Holzapfel, K. Föttinger, K. M. Neyman, G. N. Rupprechter, *J. Phys. Chem. C* **2012**, *116*, 18768.
[37] F. Gao, D. W. Goodman, *Phys. Chem. Chem. Phys.* **2012**, *14*, 6688.
[38] P. S. Cremer, X. Su, Y. R. Shen, G. A. Somorjai, *J. Am. Chem. Soc.* **1996**, *118*, 2942.
[39] P. S. Cremer, X. Su, G. A. Somorjai, Y. R. Shen, *J. Mol. Catal. A* **1998**, *131*, 225.
[40] K. M. Bratlie, H. Lee, K. Komvopoulos, P. Yang, G. A. Somorjai, *Nano Lett.* **2007**, *7*, 3097.
[41] F. Gao, Y. Wang, D. W. Goodman, *J. Am. Chem. Soc.* **2009**, *131*, 5734.
[42] H. J. Freund, G. Meijer, M. Scheffler, R. Schlögl, M. Wolf, *Angew. Chem. Int. Ed.* **2011**, *50*, 10064; *Angew. Chem.* **2011**, *123*, 10242.
[43] C. Rameshan, W. Stadlmayr, C. Weilach, S. Penner, H. Lorenz, M. Hävecker, R. Blume, T. Rocha, D. Teschner, A. Knop-Gericke, R. Schlögl, N. Memmel, D. Zemlyanov, G. Rupprechter, B. Klötzer, *Angew. Chem. Int. Ed.* **2010**, *49*, 3224; *Angew. Chem.* **2010**, *122*, 3292.
[44] H. Oosterbeek, *Phys. Chem. Chem. Phys.* **2007**, *9*, 3570.
[45] E. Ozensoy, C. Hess, D. Loffreda, P. Sautet, D. W. Goodman, *J. Phys. Chem. B* **2005**, *109*, 5414.
[46] M. K. Rose, T. Mitsui, J. Dunphy, A. Borg, D. F. Ogletree, M. Salmeron, P. Sautet, *Surf. Sci.* **2002**, *512*, 48.
[47] W. K. Kuhn, J. Szanyi, D. W. Goodman, *Surf. Sci.* **1992**, *274*, L611.
[48] H. Liu, Y. Tong, N. Kuwata, M. Osawa, J. Kawamura, S. Ye, *J. Phys. Chem. C* **2009**, *113*, 20531.
[49] X. Chen, M. L. Clarke, J. I. E. Wang, Z. Chen, *Int. J. Mod. Phys. B* **2005**, *19*, 691.

[50] P. B. Miranda, Y. R. Shen, *J. Phys. Chem. B* **1999**, *103*, 3292.
[51] Z. Chen, Y. R. Shen, G. A. Somorjai, *Annu. Rev. Phys. Chem.* **2002**, *53*, 437.
[52] G. A. Somorjai, J. Carrazza, *Ind. Eng. Chem. Res. Fundamentals* **1986**, *25*, 63.
[53] W. D. Michalak, J. M. Krier, K. Komvopoulos, G. A. Somorjai, *J. Phys. Chem. C* **2013**, *117*, 1809.
[54] K. R. McCrea, G. A. Somorjai, *J. Mol. Catal. A* **2000**, *163*, 43.
[55] M. Yang, G. A. Somorjai, *J. Am. Chem. Soc.* **2004**, *126*, 7698.
[56] S. Baldelli, N. Markovic, P. Ross, Y.-R. Shen, G. Somorjai, *J. Phys. Chem. B* **1999**, *103*, 8920.
[57] K. M. Bratlie, C. J. Kliewer, G. A. Somorjai, *J. Phys. Chem. B* **2006**, *110*, 17925.
[58] C. J. Kliewer, M. Bieri, G. A. Somorjai, *J. Phys. Chem. C* **2008**, *112*, 11373.
[59] X. Su, K. Kung, J. Lahtinen, R. Y. Shen, G. A. Somorjai, *Catal. Lett.* **1998**, *54*, 9.
[60] K. M. Bratlie, L. D. Flores, G. A. Somorjai, *Surf. Sci.* **2005**, *599*, 93.
[61] M. Yang, K. C. Chou, G. A. Somorjai, *J. Phys. Chem. B* **2004**, *108*, 14766.
[62] G. A. Somorjai, J. Y. Park, *Angew. Chem. Int. Ed.* **2008**, *47*, 9212; *Angew. Chem.* **2008**, *120*, 9352.
[63] G. A. Somorjai, C. J. Kliewer, *React. Kinet. Catal. Lett.* **2009**, *96*, 191.
[64] T. Ishida, M. Haruta, *Angew. Chem. Int. Ed.* **2007**, *46*, 7154; *Angew. Chem.* **2007**, *119*, 7288.
[65] G. B. Shul'pin, *Org. Biomol. Chem.* **2010**, *8*, 4217.
[66] I. Lee, F. Delbecq, R. Morales, M. A. Albiter, F. Zaera, *Nat. Mater.* **2009**, *8*, 132.
[67] C. J. Kliewer, C. Aliaga, M. Bieri, W. Huang, C. K. Tsung, J. B. Wood, K. Komvopoulos, G. A. Somorjai, *J. Am. Chem. Soc.* **2010**, *132*, 13088.
[68] A. G. de Beer, S. Roke, *Phys. Rev. B* **2009**, *79*, 155420.
[69] S. Roke, M. Bonn, A. V. Petukhov, *Phys. Rev. B* **2004**, *70*, 115106.
[70] S. Roke, G. Gonella, *Annu. Rev. Phys. Chem.* **2012**, *63*, 353.
[71] S. Roke, *ChemPhysChem* **2009**, *10*, 1380.
[72] S. Roke, W. G. Roeterdink, J. E. Wijnhoven, A. V. Petukhov, A. W. Kleyn, M. Bonn, *Phys. Rev. Lett.* **2003**, *91*, 258302.
[73] P. B. Miranda, V. Pflumio, H. Saijo, Y. R. Shen, *J. Am. Chem. Soc.* **1998**, *120*, 12092.
[74] S. J. Kweskin, R. M. Rioux, H. Song, K. Komvopoulos, P. Yang, G. A. Somorjai, *ACS Catal.* **2012**, *2*, 2377.
[75] C. Aliaga, J. Y. Park, Y. Yamada, H. S. Lee, C.-K. Tsung, P. Yang, G. A. Somorjai, *J. Phys. Chem. C* **2009**, *113*, 6150.
[76] M. Crespo-Quesada, J. M. Andanson, A. Yarulin, B. Lim, Y. Xia, L. Kiwi-Minsker, *Langmuir* **2011**, *27*, 7909.
[77] C. T. Williams, Y. Yang, C. D. Bain, *Langmuir* **2000**, *16*, 2343.
[78] M. S. Yeganeh, S. M. Dougal, B. G. Silbernagel, *Langmuir* **2006**, *22*, 637.
[79] G. Kennedy, L. R. Baker, G. A. Somorjai, *Angew. Chem. Int. Ed.* **2014**, *53*, 3405; *Angew. Chem.* **2014**, *126*, 3473.
[80] S. Siegbahn, C. Nordling, G. Johansson, J. Hedman, P. F. Heden, K. Hamrin, U. Gelius, T. Bergmark, L. O. Werme, R. Manne, Y. Baer, *ESCA applied to free molecules*. North-Holland Pub. Co., **1969**.
[81] H. Siegbahn, K. Siegbahn, *J. Electron. Spectrosc. Relat. Phenom.* **1973**, *2*, 319.
[82] R. W. Joyner, M. W. Roberts, K. Yates, *Surf. Sci.* **1979**, *87*, 501.
[83] A. Howie, *Proc. EMAG* **1981**, 419.
[84] H. Siegbahn, *J. Phys. Chem.* **1985**, *89*, 897.
[85] D. M. Littrell, B. J. Tatarchuk, *J. Vac. Sci. Technol. A* **1986**, *4*, 1608.
[86] H. J. Ruppender, M. Grunze, C. W. Kong, M. Wilmers, *Surf. Interface Anal.* **1990**, *15*, 245.
[87] M. Grunze, D. J. Dwyer, M. Nassir, Y. Tsai, *Surf. Sci. Catal.* **1992**, *482*, 169.
[88] D. F. Ogletree, H. Bluhm, G. Lebedev, C. S. Fadley, Z. Hussain, M. Salmeron, *Rev. Sci. Instrum.* **2002**, *73*, 3872.
[89] H. Bluhm, M. Hävecker, A. Knop-Gericke, E. Kleimenov, R. Schlögl, D. Teschner, V. I. Bukhtiyarov, D. F. Ogletree, M. Salmeron, *J. Phys. Chem. B* **2004**, *108*, 14340.
[90] D. F. Ogletree, H. Bluhm, E. D. Hebenstreit, M. Salmeron, *Nucl. Instrum. Methods* **2009**, *601*, 151.
[91] F. Tao, M. E. Grass, Y. Zhang, D. R. Butcher, J. R. Renzas, Z. Liu, J. Y. Chung, B. S. Mun, M. Salmeron, G. A. Somorjai, *Science* **2008**, *322*, 932.
[92] F. Tao, M. E. Grass, Y. Zhang, D. R. Butcher, F. Aksoy, S. Aloni, V. Altoe, S. Alayoglu, J. R. Renzas, C. K. Tsung, Z. Zhu, Z. Liu, M. Salmeron, G. A. Somorjai, *J. Am. Chem. Soc.* **2010**, *132*, 8697.
[93] K. Qadir, S. H. Joo, B. S. Mun, D. R. Butcher, J. R. Renzas, F. Aksoy, Z. Liu, G. A. Somorjai, J. Y. Park, *Nano Lett.* **2012**, *12*, 5761.
[94] N. Musselwhite, S. Alayoglu, G. Melaet, V. V. Pushkarev, A. E. Lindeman, K. An, G. A. Somorjai, *Catal. Lett.* **2013**, *143*, 907.
[95] S. K. Beaumont, S. Alayoglu, V. V. Pushkarev, Z. Liu, N. Kruse, G. A. Somorjai, *Faraday Discuss.* **2013**, *162*, 31.
[96] S. Alayoglu, S. K. Beaumont, G. Melaet, A. E. Lindeman, N. Musselwhite, C. J. Brooks, M. A. Marcus, J. Guo, Z. Liu, N. Kruse, *J. Phys. Chem. C* **2013**, *117*, 21803.
[97] M. E. Grass, Y. Zhang, D. R. Butcher, J. Y. Park, Y. Li, H. Bluhm, K. M. Bratlie, T. Zhang, G. A. Somorjai, *Angew. Chem. Int. Ed.* **2008**, *47*, 8893; *Angew. Chem.* **2008**, *120*, 9025.
[98] S. Alayoglu, K. An, G. Melaet, S. Chen, F. Bernardi, L. W. Wang, A. E. Lindeman, N. Musselwhite, J. Guo, Z. Liu, *J. Phys. Chem. C* **2013**, *117*, 26608.
[99] G. Melaet, W. T. Ralston, C. S. Li, S. Alayoglu, K. An, N. Musselwhite, B. Kalkan, G. A. Somorjai, *J. Am. Chem. Soc.* **2014**, *136*, 2260.
[100] J. Graciani, K. Mudiyanselage, F. Xu, A. E. Baber, J. Evans, S. D. Senanayake, D. J. Stacchiola, P. Liu, J. Hrbek, J. Fernández Sanz, J. A. Rodriguez, *Science* **2014**, *345*, 546.
[101] D. C. Koningsberger, D. E. Ramaker, *Handbook of Heterogeneous Catalysis*, Wiley-VCH, Weinheim.
[102] G. A. Somorjai, S. K. Beaumont, S. Alayoglu, *Angew. Chem. Int. Ed.* **2011**, *50*, 10116; *Angew. Chem.* **2011**, *123*, 10298.
[103] S. Alayoglu, J. M. Krier, W. D. Michalak, Z. Zhu, E. Gross, G. A. Somorjai, *ACS Catal.* **2012**, *2*, 2250.
[104] M. S. Nashner, A. I. Frenkel, D. L. Adler, J. R. Shapley, R. G. Nuzzo, *J. Am. Chem. Soc.* **1997**, *119*, 7760.
[105] C. W. Hills, M. S. Nashner, A. I. Frenkel, J. R. Shapley, R. G. Nuzzo, *Langmuir* **1999**, *15*, 690.
[106] H. Liu, J. Guo, Y. Yin, A. Augustsson, C. Dong, J. Nordgren, C. Chang, P. Alivisatos, G. Thornton, D. F. Ogletree, *Nano Lett.* **2007**, *7*, 1919.
[107] S. Alayoglu, P. Zavalij, B. Eichhorn, Q. Wang, A. I. Frenkel, P. Chupas, *ACS Nano* **2009**, *3*, 3127.
[108] F. Zheng, S. Alayoglu, J. Guo, V. Pushkarev, Y. Li, P. A. Glans, J. L. Chen, G. Somorjai, *Nano. Lett.* **2011**, *11*, 847.
[109] K. Föttinger, J. A. van Bokhoven, M. Nachtegaal, G. N. Rupprechter, *J. Phys. Chem. Lett.* **2011**, *2*, 428.
[110] U. Jung, A. Elsen, Y. Li, J. G. Smith, M. W. Small, E. A. Stach, A. I. Frenkel, R. G. Nuzzo, *ACS Catal.* **2015**, *5*, 1539 – 1551.
[111] H. Imai, K. Izumi, M. Matsumoto, Y. Kubo, K. Kato, Y. Imai, *J. Am. Chem. Soc.* **2009**, *131*, 6293.
[112] S. L. Shannon, J. G. Goodwin, Jr., *Chem. Rev.* **1995**, *95*, 677.
[113] V. Frøseth, S. Storsæter, Ø. Borg, E. A. Blekkan, M. Rønning, A. Holmen, *Appl. Catal. A* **2005**, *289*, 10.
[114] S. Vada, A. Hoff, E. Ådnanes, D. Schanke, A. Holmen, *Top. Catal.* **1995**, *2*, 155.
[115] A. Frennet, C. Hubert, *J. Mol. Catal. A* **2000**, *163*, 163.
[116] J. Schweicher, A. Bundhoo, N. Kruse, *J. Am. Chem. Soc.* **2012**, *134*, 16135.
[117] G. Melaet, W. T. Ralston, W.-C. Liu, G. A. Somorjai, *J. Phys. Chem. C* **2014**, *118*, 26921.
[118] C. V. Gaskell, C. M. Parlett, M. A. Newton, K. Wilson, A. F. Lee, *ACS Catal.* **2012**, *2*, 2242.
[119] L. J. Richter, T. P. Petralli-Mallow, J. C. Stephenson, *Opt. Lett.* **1998**, *23*, 1594.
[120] J. Kubota, A. Wada, K. Domen, S. S. Kano, *Chem. Phys. Lett.* **2002**, *362*, 476.
[121] V. L. Zhang, H. Arnolds, D. A. King, *Surf. Sci.* **2005**, *587*, 102.
[122] R. B. Kutz, B. Braunschweig, P. Mukherjee, R. L. Behrens, D. D. Dlott, A. Wieckowski, *J. Catal.* **2011**, *278*, 181.
[123] W. G. Roeterdink, J. F. M. Aarts, A. W. Kleyn, M. Bonn, *J. Phys. Chem. B* **2004**, *108*, 14491.
[124] L. Velarde, X. Y. Zhang, Z. Lu, A. G. Joly, Z. Wang, H. F. Wang, *J. Chem. Phys.* **2011**, *135*, 241102.
[125] M. Nagao, K. Watanabe, Y. Matsumoto, *J. Phys. Chem. C* **2009**, *113*, 11712.
[126] Y. Rao, B. Doughty, N. J. Turro, K. B. Eisenthal, *Ultrafast Infrared Vibrational Spectroscopy*, CRC Press, **2013**.
[127] G. M. Santos, S. Baldelli, *J. Phys. Chem. C* **2013**, *117*, 17591.
[128] K. A. Cimatu, S. Baldelli, *J. Phys. Chem. C* **2009**, *113*, 16575.

[129] M. Flörsheimer, M. Bösch, C. Brillert, M. Wierschem, H. Fuchs, *Adv. Mater.* **1997**, *9*, 1061.
[130] H. C. Hieu, N. A. Tuan, H. Li, Y. Miyauchi, G. Mizutani, *Appl. Spectrosc.* **2011**, *65*, 1254.
[131] Y. Han, V. Raghunathan, R. R. Feng, H. Maekawa, C. Y. Chung, Y. Feng, E. O. Potma, N. H. Ge, *J. Phys. Chem. B* **2013**, *117*, 6149.
[132] V. Raghunathan, Y. Han, O. Korth, N. H. Ge, E. O. Potma, *Opt. Lett.* **2011**, *36*, 3891.
[133] S. Kogure, K. Inoue, T. Ohmori, M. Ishihara, M. Kikuchi, M. Fujii, M. Sakai, *Opt. Express* **2010**, *18*, 13402.
[134] K. Cimatu, H. J. Moore, D. Barriet, P. Chinwangso, T. R. Lee, S. Baldelli, *J. Phys. Chem. C* **2008**, *112*, 14529.
[135] M. Hernandez, P. Chinwangso, K. Cimatu, L.-O. Srisombat, T. R. Lee, S. Baldelli, *J. Phys. Chem. C* **2011**, *115*, 4688.
[136] K. Cimatu, S. Baldelli, *J. Am. Chem. Soc.* **2006**, *128*, 16016.
[137] E. de Smit, I. Swart, J. F. Creemer, G. H. Hoveling, M. K. Gilles, T. Tyliszczak, P. J. Kooyman, H. W. Zandbergen, C. Morin, B. M. Weckhuysen, *Nature* **2008**, *456*, 222.
[138] L. R. Aramburo, S. Wirick, P. S. Miedema, I. L. Buurmans, F. M. de Groot, B. M. Weckhuysen, *Phys. Chem. Chem. Phys.* **2012**, *14*, 6967.
[139] L. R. Aramburo, Y. Liu, T. Tyliszczak, F. M. de Groot, J. C. Andrews, B. M. Weckhuysen, *ChemPhysChem* **2013**, *14*, 496.
[140] K. A. Nugent, *Adv. Phys.* **2010**, *59*, 1.
[141] M. J. Humphry, B. Kraus, A. C. Hurst, A. M. Maiden, J. M. Rodenburg, *Nat. Commun.* **2012**, *3*, 730.
[142] D. A. Shapiro, Y.-S. Yu, T. Tyliszczak, J. Cabana, R. Celestre, W. Chao, K. Kaznatcheev, A. L. D. Kilcoyne, F. Maia, S. Marchesini, *Nat. Photonics* **2014**, *8*, 765.
[143] S. B. Dierker, R. Pindak, R. M. Fleming, I. K. Robinson, L. Berman, *Phys. Rev. Lett.* **1995**, *75*, 449.
[144] T. Thurn-Albrecht, W. Steffen, A. Patkowski, G. Meier, E. W. Fischer, G. Grübel, D. L. Abernathy, *Phys. Rev. Lett.* **1996**, *77*, 5437.
[145] D. J. Hall, M. Soman, J. Tutt, N. Murray, A. Holland, T. Schmitt, J. Raabe, V. N. Strocov, B. Schmitt, *J. Instrum.* **2012**, *7*, C01063.
[146] B. C. Jacquot, M. E. Hoenk, T. J. Jones, T. J. Cunningham, S. Nikzad, *Electron Devices, IEEE Trans.* **2012**, *59*, 1988.
[147] G. Deptuch, A. Besson, P. Rehak, M. Szelezniak, J. Wall, M. Winter, Y. Zhu, *Ultramicroscopy* **2007**, *107*, 674.
[148] M. Battaglia, D. Contarato, P. Denes, D. Doering, T. Duden, B. Krieger, P. Giubilato, D. Gnani, V. Radmilovic, *Nucl. Instrum. Methods* **2010**, *622*, 669.
[149] Z. Prieskorn, C. V. Griffith, S. D. Bongiorno, A. D. Falcone, D. N. Burrows, *Nucl. Instrum. Methods* **2013**, *717*, 83.

Received: June 8, 2015
Published online on October 23, 2015